

Electronic Supplementary Information for:

Detailed-Balance Analysis of $\text{Yb}^{3+}:\text{CsPb}(\text{Cl}_{1-x}\text{Br}_x)_3$ Quantum-Cutting Layers for High-Efficiency Photovoltaics under Real-World Conditions

Matthew J. Crane, Daniel M. Kroupa, Daniel R. Gamelin *

Department of Chemistry, University of Washington, Seattle, WA 98195-1700

*Email: gamelin@chem.washington.edu

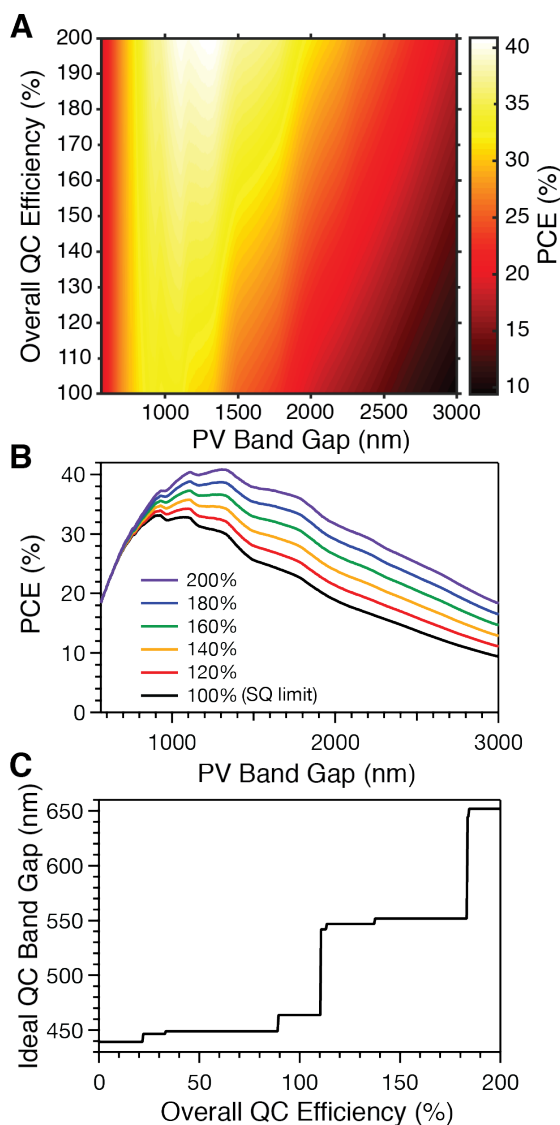


Figure S1. The data from Figure 2 converted to nm for convenience.

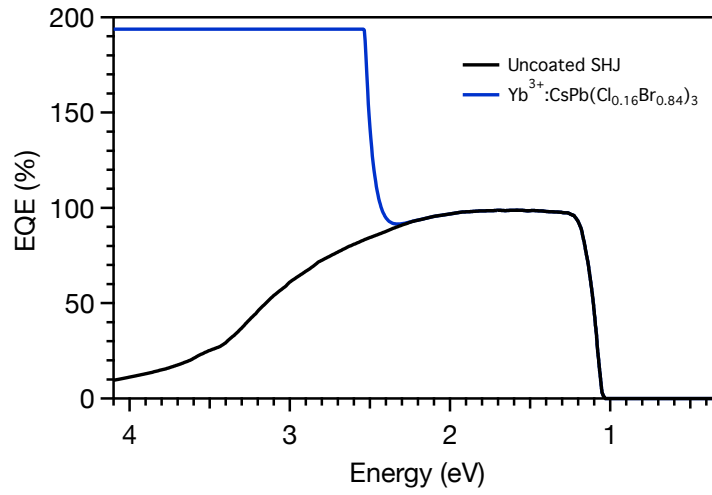


Figure S2. The predicted EQE of a $\text{Yb}^{3+}:\text{CsPb}(\text{Cl}_{0.16}\text{Br}_{0.84})_3/\text{SHJ}$ QC/PV device. Here, η is 200%. This provides a visual representation of the integrand of eq 4.

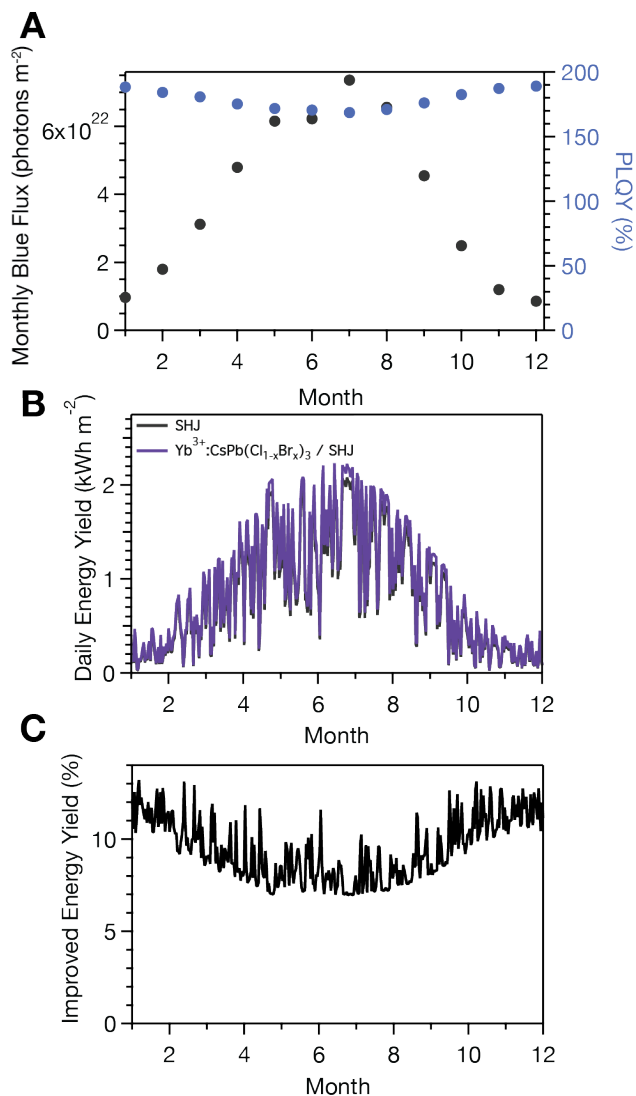


Figure S3. The effect of saturation on $\text{Yb}^{3+}:\text{CsPb}(\text{Cl}_{0.16}\text{B}_{0.84})_3$ PLQY and energy yield on $\text{Yb}^{3+}:\text{CsPb}(\text{Cl}_{0.16}\text{B}_{0.84})_3/\text{SHJ}$ device averaged on a day time scale for a TMD in Seattle, WA. **(A)** The total monthly flux blue flux integrated from 4.133 to 2.531 eV (300 to 490 nm), and the average monthly PLQY during hours of power generation. **(B)** A comparison of the daily energy yield produced by a SHJ device and a $\text{Yb}^{3+}:\text{CsPb}(\text{Cl}_{0.16}\text{B}_{0.84})_3/\text{SHJ}$ device and **(C)** the improved daily energy yield.

Two-axis tracking Seattle, WA

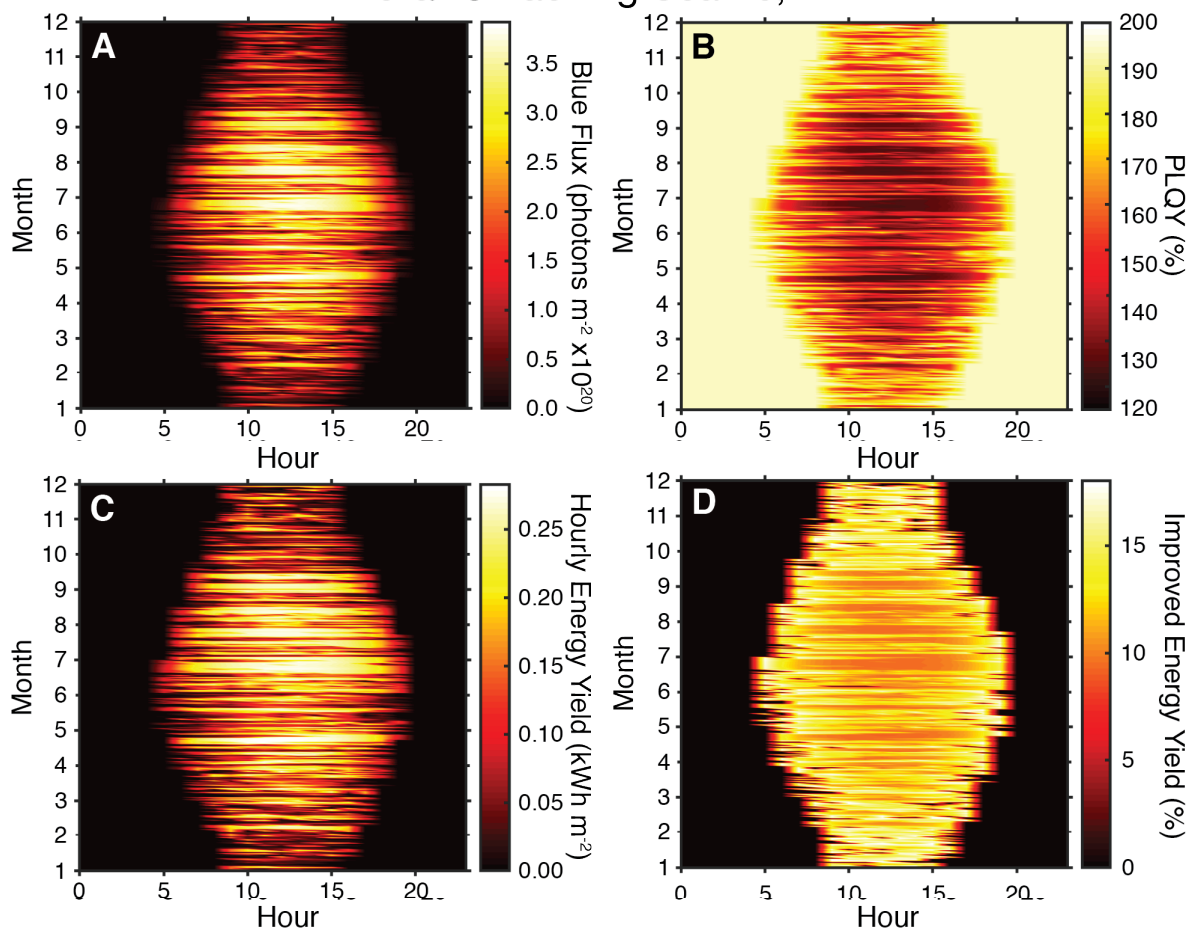


Figure S4. The impact of flux-dependent quantum yields for a $\text{Yb}^{3+}:\text{CsPb}(\text{Cl}_{0.16}\text{Br}_{0.84})_3/\text{SHJ}$ QC/PV device, represented for a typical meteorological year in Seattle, WA, USA, using two-axis tracking.¹ **(A)** The average hourly, global horizontal irradiance (GHI) photon flux from 300 to 490 nm absorbed by an optimized $\text{Yb}^{3+}:\text{CsPb}(\text{Cl}_{1-x}\text{Br}_x)_3$ quantum cutter. **(B)** The hourly PLQY of the QC material using the data from panel (A) and experimental PL saturation results from ref. 2. **(C)** The areal hourly energy yield of the QC/PV device, calculated using the model from Figure 4 and assuming 100% optical coupling of the QC PL. **(D)** The corresponding percent increase in areal hourly energy yield relative to a standard SHJ PV without a QC layer, in Seattle with two-axis tracking.

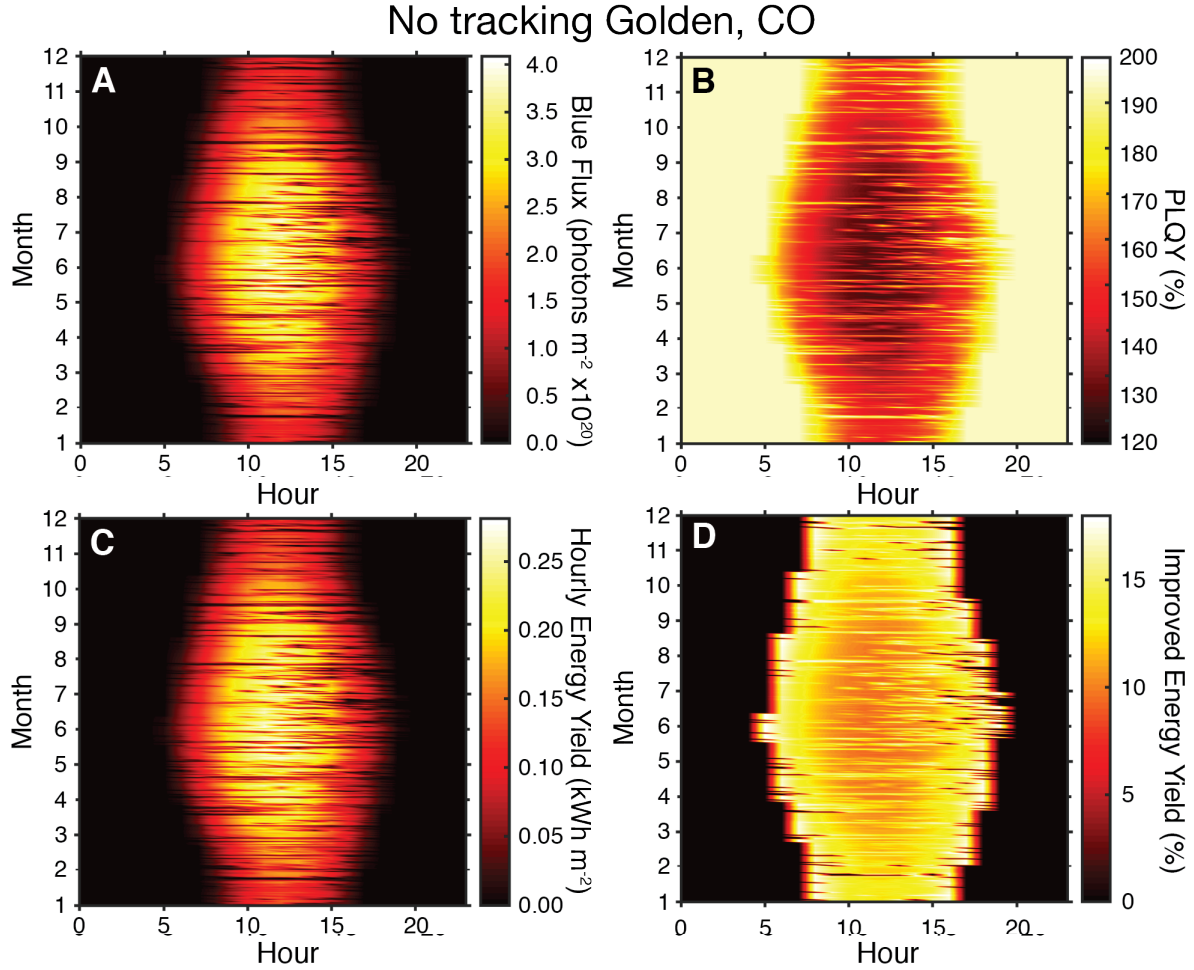


Figure S5. The impact of flux-dependent quantum yields for a $\text{Yb}^{3+}:\text{CsPb}(\text{Cl}_{0.16}\text{Br}_{0.84})_3/\text{SHJ}$ QC/PV device, represented for a typical meteorological year in Golden, CO, USA, without tracking.¹ (A) The average hourly, global horizontal irradiance (GHI) photon flux from 300 to 490 nm absorbed by an optimized $\text{Yb}^{3+}:\text{CsPb}(\text{Cl}_{1-x}\text{Br}_x)_3$ quantum cutter. (B) The hourly PLQY of the QC material using the data from panel (A) and experimental PL saturation results from ref. 2. (C) The areal hourly energy yield of the QC/PV device, calculated using the model from Figure 4 of the main text and assuming 100% optical coupling of the QC PL. (D) The corresponding percent increase in areal hourly energy yield relative to a standard SHJ PV without a QC layer, in Colorado.

Two-axis tracking Golden, CO

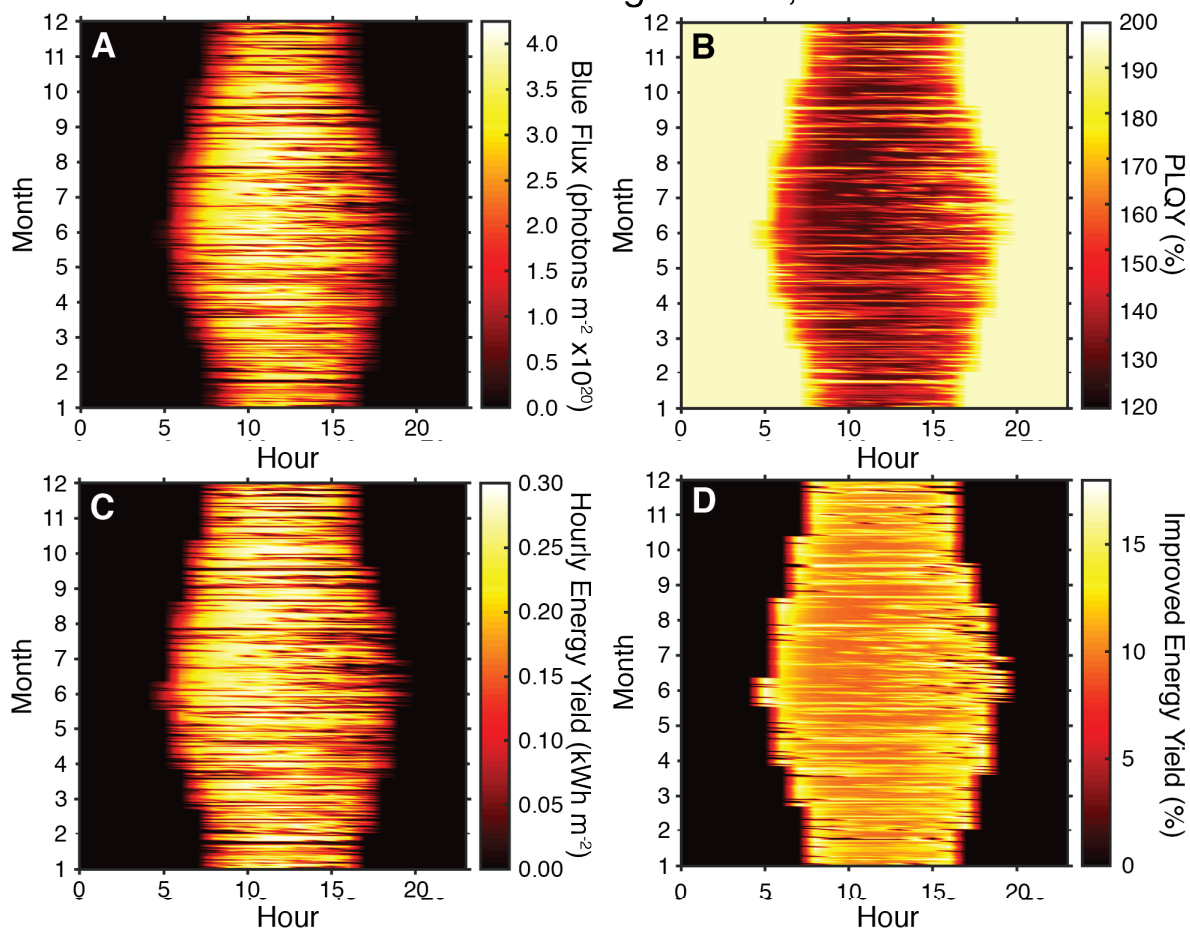


Figure S6. The impact of flux-dependent quantum yields for a $\text{Yb}^{3+}:\text{CsPb}(\text{Cl}_{0.16}\text{Br}_{0.84})_3/\text{SHJ}$ QC/PV device, represented for a typical meteorological year in Golden, CO, USA, using two-axis tracking.¹ **(A)** The average hourly, global horizontal irradiance (GHI) photon flux from 300 to 490 nm absorbed by an optimized $\text{Yb}^{3+}:\text{CsPb}(\text{Cl}_{1-x}\text{Br}_x)_3$ quantum cutter. **(B)** The hourly PLQY of the QC material using the data from panel (A) and experimental PL saturation results from ref. 2. **(C)** The areal hourly energy yield of the QC/PV device, calculated using the model from Figure 4 of the main text and assuming 100% optical coupling of the QC PL. **(D)** The corresponding percent increase in areal hourly energy yield relative to a standard SHJ PV without a QC layer, in Colorado with two-axis tracking.

Table S1. Collection of symbols, their meanings, and their units used in the calculation.

Symbol	Meaning	Unit
PCE	Device power conversion efficiency	%
P_{device}	Areal power generated by a device	$W m^{-2}$
P_{sun}	Areal power from the sun incident on a device	$W m^{-2}$
J_{op}	Operating current density	$A m^{-2}$
V_{op}	Operating voltage	V
$\Phi_{AM1.5G}$	One-sun solar spectral irradiance	$W m^{-2} eV^{-1}$
E	Energy, typically of photons	eV
n	Refractive index	-
h	Planck's constant	J s
c	Speed of light	$M s^{-1}$
q	Elementary charge of an electron	C
V	Voltage	V
T	Temperature	K
α_{PV}	Photovoltaic absorption probability	-
α_{QC}	Quantum cutter absorption probability	-
$\bar{\alpha}_{PV}$	Photovoltaic absorption probability weighted by quantum cutter photoluminescence linewidth	-
E_{QC}	Energy of quantum cutter emission	eV
ϕ	Photoluminescence quantum yield (PLQY)	-
ξ	Efficiency of optical coupling between the quantum cutter and photovoltaic	-
η	Overall quantum cutting efficiency	-
I_{QC}	Normalized spectra line shape of the quantum cutter's photoluminescence	-

- 1 M. Sengupta, Y. Xie, A. Lopez, A. Habte, G. Maclaurin and J. Shelby, *Renewable and Sustainable Energy Reviews*, 2018, **89**, 51–60.
- 2 C. S. Erickson, M. J. Crane, T. J. Milstein and D. R. Gamelin, *J. Phys. Chem. C*, DOI:10.1021/acs.jpcc.9b01296.